Environ. Sci. Technol. **1998**, *32,* 1604−1608

Rate-Limited Sorption of Hydrophobic Organic Compounds by Soils with Well-Characterized Organic Matter

JOSEPH J. PIATT† AND MARK L. BRUSSEAU*

Soil, Water and Environmental Science, Hydrology and Water Resources, University of Arizona, 429 Shantz, Tucson, Arizona 85721

This study is focused on the rate-limited sorption of homologous series of polycyclic aromatic hydrocarbons, alkylated benzenes, chlorinated benzenes, and chlorinated alkenes by two soils, one in which the organic matter is dominated by humic acid and the other by fulvic acid. The solutes sorbed more strongly to the humic-dominated soil than the fulvic-dominated soil. The first-order molecular connectivity index ($^1X^v$), a molecular solute descriptor, provided slightly better correlations with equilibrium sorption coefficients than did the octanol−water partition coefficient (K_{ow}), an empirical solute descriptor. Thus, sorbate shape/structure may have a secondary influence on the overall magnitude of equilibrium sorption. However, sorbate shape/structure exhibited a significant influence on sorption kinetics. Distinct differences were observed in the correlations of mass-transfer coefficients to $^1X^v$ for the two soils. The differences were attributed to both sorbate shape/structure and the quantity (path length) and morphology of soil organic matter.

Introduction

Sorption plays an important role in the transport, fate, and remediation of organic pollutants in the subsurface. Modeling the movement of chemicals in the subsurface requires reliable estimates of transport parameters such as equilibrium distribution coefficients (K_d) and desorption rate coefficients (k_2). As documented by numerous studies, the sorption of organic chemicals by soils and aquifer materials is often, to a large degree, controlled by soil organic matter (SOM). This appears to be true even for natural sorbents with organic carbon contents of less than 0.1% (*1*−*3*). The interaction between hydrophobic organic compounds (HOCs) and SOM has been studied extensively (*4*−*9*). Soil organic matter also plays an important role in sorption kinetics (*3, 10*−*16*).

Several conceptual models have been developed to describe how organic chemicals are sorbed by SOM. The octanol−water model was one of the first analogues developed for SOM and has been used most frequently. This model assumes that the same processes/mechanisms that affect the partitioning of HOC between octanol and water are also the same factors controlling the partitioning of HOC between SOM and water (*4*). Reversed-phase liquid chromatography (RPLC) coatings, such as C-1, C-2, C-8, C-18, and phenyl groups, have also been used as analogues of SOM (*17, 18*). Reversed-phase liquid chromatography studies have also been done using humic acids immobilized onto silica and alumina substrates (*19*−*21*).

The models discussed above have provided a means by which to interpret and predict sorption of HOCs by SOM. While they have been used with relative success to characterize the thermodynamics of sorption, the models are not capable of describing rate-limited sorption phenomena. For this, attention has focused on models that are based on permeation/diffusion in polymers. The use of polymers as an analogue for SOM is based upon the recognition that many components of SOM are polymeric in nature. The gel partition model is based on the assumption that humic substances are highly branched polymer chains that form a 3-dimensional, randomly oriented network, a polymeric gel (*12*). For this model, the maximum rate of desorption coincides with the maximum extent of gel swelling. Thus, desorption rates are diffusion limited if the gel is only partially swollen. The intraorganic matter diffusion (IOMD) model proposed by Brusseau et al. (*15*) is based on the assumption that SOM is a flexible, cross-linked, branched, amorphous, polyelectrolytic, polymeric, organic substance within which sorbates could diffuse. The influence of sorbate, sorbent, and solvent properties on the rate-limited sorption of HOCs by soils and aquifer materials was successfully interpreted using the "IOMD" model (*15, 22*−*24*). Recently, rate-limited sorption models based on diffusion of HOCs in SOM have been proposed by additional investigators (*10, 25*−*27*). The influence of SOM heterogeneity has been discussed, with the lowest diffusion rates assumed to correspond with condensed-phase organic matter.

A major limitation of many previous analyses of sorption of HOCs by SOM is that the effect of structural properties of the solute were not considered. For example, empirical linear free energy relationships (LFERs) are generally used to describe sorption phenomenology, such as the $\log K_{oc} - \log K_{ow}$ and $\log K_{oc} - \log S_w$ (S_w, aqueous solubility) relationships (*6, 7*). The K_{ow} and S_w descriptors characterize the behavior of the solute in a solvated environment, which masks the effect of the solute itself on its sorption behavior. However, sorbate structure has been reported to have a significant influence on the degree of rate-limited sorption a compound exhibits (*15, 23, 28*). Quantitative structure−activity relationships (QSARs), based on molecular solute descriptors, have been used to examine the effect of solute size and shape on sorption equilibria (*29*−*32*) and sorption kinetics (*24, 33*). These studies successfully correlated molecular topological properties, such as molecular connectivity, to the sorption of a broad range of hydrophobic and hydrophilic organic compounds to natural soils and sediments. In fact, the QSAR approach outperformed the conventional, empirically derived LFER equations.

In this study, we investigated the effect of SOM properties and sorbate structure on the magnitude and rate of sorption of four homologous series of chlorinated alkenes, chlorobenzenes, alkylbenzenes, and polycyclic aromatic hydrocarbons by two well-characterized soils. Both soil samples were collected from the same borehole, but at different depths. These soils are distinct in that the soil from the upper interval contains SOM dominated by particulated humic materials and the soil from the lower interval contains a layered fulvic material. For the solutes of interest, magnitudes of sorption and rates of desorption between two soil types are evaluated using QSAR to examine the influence of solute structural characteristics on sorption dynamics.

* Corresponding author, Soil, Water and Environmental Science, Hydrology and Water Resources. Fax: 520-621-1647; e-mail: brusseau@ag.arizona.edu.

† Soil, Water and Environmental Science.

S0013-936X(97)00461-6 CCC: $15.00
Published on Web 04/24/1998

TABLE 1. Physical/Chemical Properties of the Sorbates

compound[a]	mass (g/mol)	solubility[b] (mg/L)	C_o[c] (mg/L)	log K_{ow}[d]	^1X[e]
benzene	78.1	1780	100	2.13	2.000
naphthalene	128.2	110	15	3.37	3.405
phenanthrene	178.2	6.2	0.50	4.57	4.815
pyrene	202.3	2.6	0.067	5.18	5.559
toluene	92.1	515	100	2.69	2.411
ethylbenzene	106.2	152	75	3.13	2.971
m-xylene	106.2	160	80	3.20	2.824
chlorobenzene	112.6	484	100	2.80	2.476
1,4-dichlorobenzene	147.0	157	40	3.40	3.025
1,2,3-TCB	181.4	40	9.5	4.10	3.544
trichloroethene	131.4	1100	75	2.53	2.075
tetrachloroethene	165.8	150	40	2.88	2.514

[a] See abbreviations for compounds in Materials and Methods section. [b] Subcooled liquid aqueous solubility values (*34*). [c] Initial solute concentration. [d] Octanol−water partition coefficients (*34*). [e] First-order valence molecular connectivity index (*35*).

Experimental Section

Sorbates and Electrolytes. Analytical-grade benzene (BNZ), naphthalene (NAP), phenanthrene (PHN), pyrene (PYR), toluene (TOL), ethylbenzene (eBNZ), *m*-xylene (mXYL), chlorobenzene (CB), 1,4-dichlorobenzene (DCB), 1,2,3-trichlorobenzene (TCB), trichloroethene (TCE), and tetrachloroethene (PCE) were purchased from Aldrich Chemical Co., Milwaukee, WI. The physical/chemical properties of these compounds are summarized in Table 1. The aqueous solubility varies over 3 orders of magnitude, as do the K_{ow} values. Values of the first-order valence molecular connectivity ($^1X^v$), which is a measure of the solute's topological size, shape, and degree of branching, ranged from 2 to 6. The connectivity values are calculated by starting with a carbon−hydrogen skeleton and adding weighted values for substituents added onto the skeleton (*35*).

Stock solute solutions were made in methanol and spiked into synthetic groundwater solutions to produce final concentrations of approximately 5−50% of the solute's aqueous solubility (Table 1). The fraction of methanol in the aqueous solutions was always less than 0.05%, which was assumed to not affect the solubility or sorption of the solutes (*36*). The synthetic groundwater solution was composed of 588 mg/L $CaCl_2 \cdot 2H_2O$, 669 mg/L $MgCl_2 \cdot 6H2O$, 127 mg/L NaCl, and 19 mg/L KCl, which matched the major cation content of the groundwater.

Sorbents. The two sandy aquifer sediment samples, SB13-5 and SB13-9, used in these experiments were cored from an uncontaminated zone at a fuel spill site in Michigan (*37*). They were collected from the same borehole, but at different depth intervals. The core materials were air-dried at room temperature, passed through a 2 mm sieve, split into subsamples using a precision sample splitter, and refrigerated in glass jars. The soil properties are summarized in Table 2.

The type of SOM was determined by base extraction of the aquifer material followed by acidification of the base soluble supernatant. By definition, the base soluble fraction contained both humic acid and fulvic acid, and the humic acid precipitated out upon acidification. Isolates of the humic and fulvic acid fractions were analyzed for C, H, N, O, P, S, and ash content (Table 2). The upper interval contained predominately humic material and the lower interval contained predominately fulvic material. The soil containing the humic material had 3.4 times more organic carbon than the soil containing the fulvic material.

The morphology of the SOM was examined using scanning electron microscopy and white light and fluorescence microscopy (*37*). The micrographs revealed organic coatings

TABLE 2. Soil and Column Properties

soil properties	SB13-5	SB13-9
depth interval (m)	1.22−1.34	1.77−1.92
sand (%)	96.3	96.3
silt (%)	0.0	1.8
clay (%)	3.7	1.9
organic carbon (g/g)	0.004 72	0.001 40
morphology	particulated	layered
predominant organic matter type	humic acid	fulvic acid
C	53.18	50.88
H	5.20	4.37
O	38.15	42.73
N	2.47	1.36
S	0.52	0.45
P	0.48	0.21
column properties		
length (cm)	7.00	7.00
bulk density (g/cm^3)	1.70	1.77
vol water content	0.36	0.34
peclet number	61(43)[a]	70(46)[b]

[a] Standard deviation ($n = 3$). [b] Standard deviation ($n = 4$).

embedded with fine particles of mineral matter. The samples were distinct in that the upper interval, SB13-5, contained a particulated (humic) material and the lower interval, SB13-9, contained a layered, or coated, (fulvic) material. The layered fulvic organic matter contained desiccation cracks and holes. The thickness of the organic matter coating for the layered fulvic soil was estimated to be ~20 μm thick, based on depth estimates from these cracks and holes to the mineral surface.

Column Methodology. Single-solute, miscible-displacement experiments were performed at room temperature at pore water velocities of approximately 37 cm h^{-1}. The column, fittings, and tubing were all made of stainless steel. The columns were wet packed with the soil of interest and flushed with synthetic groundwater solution until completely saturated. The properties of the packed columns are listed in Table 2.

The solution containing the compound of interest was pumped into the column until complete breakthrough occurred, except for phenanthrene and pyrene, and then the column was flushed with artificial groundwater solution until there was no measurable concentration of compound detected in the effluent. The phenanthrene and pyrene experiments were not continued until complete breakthrough ($C/C_o = 1$) because of extremely large retardation. Influent concentrations remained constant over the course of the solute pulse. The effluent solution pH remained constant at approximately 5.5. For most of the solutes, the column effluent was measured using a flow-through UV detector (Gilson). Phenanthrene and pyrene were fraction collected in glass screw cap centrifuge tubes (Kimax). The aqueous fractions were analyzed within 1−5 h of collection using a fluorescence spectrophotometer (Hitachi F-2000).

Data Analysis

The measured breakthrough curves were analyzed using a two-domain sorption model formulated in conjunction with the 1-dimensional advective-dispersive transport equation assuming steady-state water flow, homogeneous porous medium, and nonlinear, rate-limited sorption (*38*):

$$\frac{\rho_b}{\theta_w}\frac{\partial S_2}{\partial t} + \left(1 + \frac{\rho_b}{\theta_w} F K_f N C^{N-1}\right)\frac{\partial C}{\partial t} = D\frac{\partial^2 C}{\partial x^2} - v\frac{\partial C}{\partial x} \quad (1)$$

$$\frac{\partial S_2}{\partial t} = k_2[(1 - F)K_f C^N - S_2] \quad (2)$$

where ρ_b (M L^{-3}) is the bulk density, θ_w is the volumetric water content, F is the fraction of instantaneous sorption, K_f (L^{3N} M^{-N}) is the Freundlich sorption constant, N is the Freundlich exponent constant, C (M L^{-3}) is the aqueous solute concentration, t (T) is time, D (L^2 T^{-1}) is the dispersion coefficient, x (L) is distance, v (L T^{-1}) is pore water velocity, S_2 (M M^{-1}) is the sorbed-phase concentration for the rate-limited domain, and k_2 (T^{-1}) is the desorption rate coefficient.

A nonlinear, least-squares optimization program (FITNLNE) was used to solve the transport equation described above, which has six parameters. Three parameters were determined independently: Peclet ($P = nL/D$) values were determined from nonsorbing tracer experiments, the volume of the input pulse was measured gravimetrically, and retardation factors (R) were determined by moment analysis. The global retardation factor is defined as $R = 1 + (\rho_b/\theta_w)K_f{C_o}^{N-1}$, where C_o (M L^{-3}) is the initial aqueous solute concentration. Thus, K_d (L^3 M^{-1}) = $K_f{C_o}^{N-1} = (R - 1)\theta_w/\rho_b$. The two nondimensional parameters in which F and k_2 are embedded were optimized, as was N. Optimizations that resulted in N values close to unity ($N > 0.85$) yielded values of F and k_2 that were within 20% of the values obtained using CFITIM (*39*), a model based on linear, rate-limited sorption.

As mentioned previously, the breakthrough curves presented herein were obtained using a flow-through UV system with a lower detection limit (LDL) of approximately 0.5 mg/L. The column experiments were repeated for TCE using GC/ECD for analysis, which has a LDL of approximately 1.4 μg/L. Thus, the "tail" portion of the breakthrough curve was resolved in much greater detail. This tail portion represents less than 0.5% of the total mass of TCE introduced into and recovered from the column. The two-domain sorption model (eqs 1 and 2) could not fit the extended data. However, a model incorporating a log-normal distribution of rate coefficients provided a good fit, yielding a mean and variance for the rate coefficient. Interestingly, the mean rate coefficient for the fulvic soil was about 10 times smaller than that for the humic soil, which is opposite of what was observed for the higher concentration UV data. Thus, it appears that the mechanism influencing desorption at very low concentrations (i.e., when only a small fraction of the initial mass remains in the system) may differ from that influencing the desorption of the majority of solute mass. In this work, we will focus on the behavior of the latter.

Results and Discussion

Equilibrium Sorption. Pentafluorobenzoic acid (PFBA) was used as a nonsorbing tracer to define the hydrodynamic characteristics of the column systems. Duplicate experiments with PFBA yielded virtually identical breakthrough curves, which were sharp and symmetrical and had retardation factors equal to 1. The breakthrough curves for the sorbing solutes exhibited varying degrees of asymmetry and tailing, which indicated that the nonideality was caused by a sorption-related rather than transport-related mechanism. Representative breakthrough curves for the sorbing solutes are shown in Figure 1, along with the optimized simulations.

For each homologous series of compounds, the extent of sorption increased as the solubility of the chemical decreased, as expected, with K_d values ranging over 3 orders of magnitude. For both soils, K_d correlated well to K_{ow} and ${}^1X^v$, with ${}^1X^v$ providing a slightly better correlation coefficient (*40*). This indicates that the gross size of the solute had a large, primary effect on equilibrium sorption, as would be expected for a process that is controlled by entropic solute/aqueous solution interactions. In such cases, there should be a correlation between sorption and any descriptor/parameter that reflects this entropically driven process. However, the fact that ${}^1X^v$ provided a better correlation suggests that the shape and degree of branching of the solute had a small, secondary effect on equilibrium sorption for this aqueous/soil system. If sorption was controlled only by the activity of solutes in solution, then K_d and K_{ow} should be perfectly correlated, which they are not. In addition, it is known that K_{oc} values vary from soil to soil, which indicates that solute−sorbent interactions influence equilibrium sorption behavior. Thus, a parameter such as ${}^1X^v$ may be more appropriate for characterizing sorption given that solute-sorbent interactions are usually important.

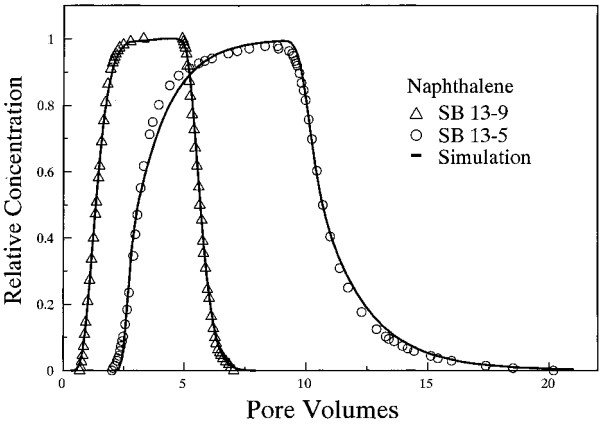

FIGURE 1. Measured and simulated breakthrough curves for naphthalene transport in the humic soil (SB-5) and in the fulvic soil (SB-9).

TABLE 3. Rate Coefficients and Mass Transfer Coefficients[a]

	interval SB13-5			interval SB13−9		
solute	n_5	k_2 (h^{-1})	α (h^{-1})	n_9	k_2 (h^{-1})	α (h^{-1})
BNZ	5	20.1 (18.1)	5.51 (6.98)	3	17.7 (8.6)	11.0 (5.2)
NAP	7	7.67 (1.72)	5.09 (1.19)	3	17.2 (8.8)	7.87(4.36)
PHN	2	0.185 (0.038)	0.0888 (0.0330)	2	0.769 (0.103)	0.334 (0.075)
PYR	1	0.0403 (0.0021)	0.0236 (0.0016)	1	0.114 (0.005)	0.0487 (0.0024)
TOL	2	23.9 (3.8)	8.17 (1.38)	1	9.91 (1.16)	5.75(0.67)
eBNZ	1	10.6 (0.9)	6.07 (0.61)		ND[b]	ND
mXYL	1	16.5 (2.8)	7.43 (1.29)		ND	ND
CB	2	20.8 (7.5)	9.33 (3.37)	1	17.6 (2.06)	6.91(1.05)
DCB	2	11.4 (2.3)	9.30 (2.09)		ND	ND
TCB	2	3.44 (0.34)	1.93 (0.21)	2	13.8 (2.3)	8.20(1.41)
TCE	1	19.2 (0.1)	5.64 (0.56)		ND	ND
PCE	1	11.7 (0.8)	4.32 (0.8)		ND	ND

[a] Values in parenthesis are error estimates (±1 s). Error estimates were calculated based on the standard deviations calculated by the optimization program (CFITIM) and propagating them through subsequent calculations. [b] Not determined.

Rate-Limited Sorption. If rate-limited sorption is controlled by intraorganic matter diffusion, as assumed herein, then the solute's size, shape, and degree of branching should influence its rate behavior. Quantitative structure−activity relationships (QSARs) can be used to relate sorption kinetics properties, such as mass transfer coefficients, directly to the molecular properties of a solute. The first-order, reverse-sorption rate constant (k_2) can be related to a mass transfer coefficient (α, s^{-1}) and an intrasorbent diffusion coefficient (D, cm^2 s^{-1}) by

$$\alpha = k_2(1 - F) = \frac{aD}{l^2} \qquad (3)$$

where a is the diffusion domain shape factor and l (L) is the characteristic diffusion length (*24*).

A plot of log α (Table 3) versus ${}^1X^v$ for both soils is shown in Figure 2 (see caption for regression equations). Mass-transfer coefficients were relatively similar in magnitude for

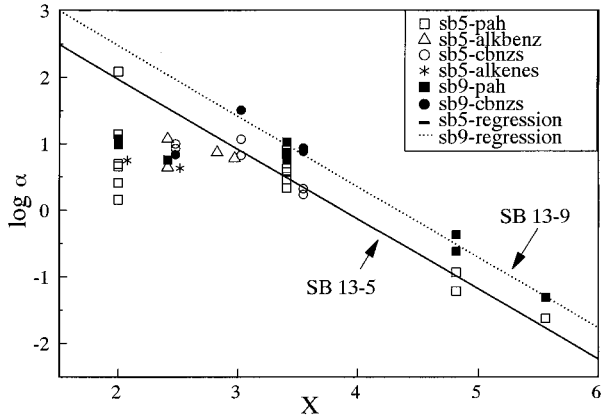

FIGURE 2. Correlation between the log of the mass transfer coefficient (α, h^{-1}) and the first-order valence molecular connectivity ($^1X^v$) index for both soils. The regressions are for solutes with $^1X^v > 2$ only SB-5, log $\alpha = -1.05\ ^1X^v + 4.07$ ($r^2 = 0.98$, $n = 11$); SB-9, log $\alpha = -1.06\ ^1X^v + 4.59$ ($r^2 = 0.98$, $n = 9$).

solutes with $^1X^v < 2$ and decreased logarithmically for $^1X^v > 2$. The flat portion of the curve corresponded to the smaller, more soluble HOCs. One possible explanation for this behavior is that these solutes, which are 0.2−0.5 nm in diameter, may have relatively unhindered movement within the SOM matrix.

The α values for the solutes with $^1X^v > 2$ were log-linearly correlated to the solute molecular descriptor, as observed previously (*24, 33*). No distinction in α values were observed between the families of compounds, indicating that $^1X^v$ described the mass-transfer behavior for all the HOCs. This may not be the case for more reactive solutes. The regressions in Figure 2 were similar to the regression reported by Hu and co-workers (*33*) for sorption of HOCs by a low organic carbon aquifer material (log $\alpha = -1.02\ ^1X^v + 4.31$; $r^2 = 0.88$; $n = 15$). The slopes are nearly identical between the two studies, with differences only in the intercept values. In both cases, the mass transfer coefficients vary over 300 times, while the aqueous diffusion coefficients for the solutes vary only 2−3 times. This is consistent with a mechanism involving constrained diffusion within SOM.

For this study, the log $\alpha/^1X^v$ relationships for both soils had essentially equivalent slopes, but different intercepts. The α values for the fulvic soil were, on average, 3.3 times greater than the α values for the humic soil, based on the difference in intercept values for the two regressions. This measured difference in α values could be attributed to differences in one or more of the following factors: intrasorbent diffusion coefficient, diffusion path length, or shape factor (eq 3). The difference in α values may be due to differences in diffusion coefficients for a given sorbate, reflecting differences in "polymeric structure" between fulvic acids and humic acids. Given the properties of the two, the fulvic material should be more hydrated, water soluble, and flexible in nature than the humic material. If this is true, then the α values for sorption by the fulvic soil should be larger because solute diffusion within the organic matrix would be less restricted. However, equivalent slope values for the log $\alpha/^1X^v$ relationship may indicate that the intrasorbent diffusion coefficients (D) for a given solute are similar for both soils, especially considering both soils have the same parent organic material. Furthermore, differences in D values are expected to be very small between humic and fulvic materials compared to differences between the broad range of SOM components (e.g., lipids versus shale). Thus, the following analysis will be based on the assumption that D values are equivalent for both soils.

The potential contribution of differences in diffusion path lengths to the differences in α values can be evaluated initially by assuming that $a_1 = a_2$ and $D_1 = D_2$. In this case, we have $\alpha_1/\alpha_2 = (l_2/l_1)^2$ from eq 3. The measured $\alpha_{SB-9}/\alpha_{SB-5}$ ratio of 3.3 corresponds to an l_5/l_9 ratio of 1.8. Thus, the diffusion path length for the particulated humic soil is estimated to be 1.8 times longer than that for the layered fulvic soil, assuming all associated assumptions are valid. The average diffusion path length for the particulated humic soil is estimated to be 18 μm, for an average total thickness of 36 μm, given the measured thickness of 20 μm for the layered fulvic material.

TABLE 4. Intraorganic Matter Diffusion Coefficients (10^{10} cm^2 s^{-1})

solute	SB13-5	SB13-9	Lemmon[a]	Borden[b]
BNZ	25.9	16.3	1.84	1.88
NAP	15.4	9.54	0.016	0.11
PHN	0.418	0.495		
PYR	0.111	0.0721		0.000 44
TOL	38.4	8.51	1.70	1.06
eBNZ	28.6			1.37
mXYL	35.0			0.456
CB	43.9	10.2	0.842	1.63
DCB	43.7			
TCB	9.08	12.1		0.125
TCE	26.5		0.724	1.01
PCE	20.3		0.215	0.118

[a] Reference 33: $l = 11.5$ um, $c = 1.876$. [b] Reference 33: $l = 1.0$ um, $c = 1.876$.

The above analysis is based on an assumption that the SOM for the two soils have identical morphologies. However, the SEM analysis showed that the fulvic material occurred as a relatively continuous coating, whereas the humic material existed as discrete chunks and patches on the grain surfaces. This suggests that the morphologies are not identical. The morphology of the SOM is represented by the shape factor (a) in eq 3. Shape factor values for solutes diffusing into porous domains of different geometries have been determined (*41*). The fulvic soil, with the layered organic coating, is assumed to have a plane-sheet geometry. At a molecular scale, the soil surface is viewed as a flat plane coated with a sheet of organic matter through which solutes diffuse. The shape-factor value for a plane sheet is 1.876. The particulated chunks or patches of organic matter associated with the humic soil are assumed to have a solid cylinder geometry with the cylinder length equal to its diameter. The shape-factor value for a solid cylinder with these dimensions is 4.630. The calculated shape factors can be used with the measured $\alpha_{SB-9}/\alpha_{SB-5}$ ratio to estimate the path length ratio (l_5/l_9), which is 2.8. This equates to a path length of 28 μm for the humic soil, given the measured path length value of 10 μm for the fulvic soil.

The above analysis results in an estimated equivalent thickness of 57 μm for the humic material, compared to a thickness of 36 μm when the shape factors were assumed equal for the humic and fulvic soils. The fulvic soil had a measured organic coating thickness of 20 μm. Hu et al. (*33*) calculated effective diffusion path lengths of 1 μm for Borden aquifer material and 11 μm for Mt. Lemmon surface soil. Holmen and Gschwend (*26*) reported organic coating thicknesses ranging from 10 to 100 μm for three different sandy aquifer materials. The path lengths reported in our study are consistent with the findings of both these studies.

Diffusion coefficients were calculated for the solutes using the path lengths (humic, 28 μm, and fulvic, 10 μm) and shape factors (humic, 4.630, and fulvic, 1.876) given above (Table 4). The D values for a given solute are approximately 5 orders of magnitude smaller than their corresponding aqueous diffusion coefficients and span a range of more than 3 orders of magnitude for different solutes. In contrast, aqueous

diffusion coefficients vary approximately 2−3 times for these solutes. This indicates diffusion is highly restricted within the SOM matrix and is very dependent on the size and shape of the diffusing solute. The *D* values for a given solute were similar between the two soils. This supports the previous assumption that differences in mass transfer coefficients were due to differences in diffusion path lengths and shape factors, and not significant differences in the properties of the SOM, such as degree of cross-linking.

The diffusion coefficients for the most soluble HOCs (benzene, toluene, CB, DCB, and TCE) were in the order of 1×10^{-9} cm^2 s^{-1}. These *D* values were 10−20 times larger than those reported for sorption of similar HOCs by Borden aquifer material and Mt. Lemmon soil (*33*). These differences may be due to the fact that the diffusion path lengths for the Borden and Mt. Lemmon material were estimated by assuming the SOM was evenly distributed (as a shell) over the porous media.

Diffusion coefficients for similar compounds in synthetic-polymer systems are in the order of 2×10^{-8} cm^2 s^{-1} for styrene-butadiene rubber (*42*), 1×10^{-7} cm^2 s^{-1} for polyurethane (*43*), and 2×10^{-6} cm^2 s^{-1} for silicone rubber (*44*). Thus, diffusion coefficients for the polymer systems are 10−1000 times larger than for the natural SOM. The densities (g cm^{-3}) of the polymers are 1.13 (styrene-butadiene rubber), 0.85 (polyurethane), and 1.09 (silicone rubber) (*42, 45, 46*). The density of SOM has been estimated to range from 1.2 to 1.4 g cm^{-3} (*37, 47, 48*). The fact that SOM is slightly more dense than these synthetic polymers may partially explain the observation that diffusion in the SOM was more constrained than in the polymers. In addition, the more complex, heterogeneous nature of SOM may cause greater constraints to diffusive flux. Thus, the morphology of the diffusion domain is likely to be important in natural SOM systems. In addition to sorbent shape and thickness, solute structure is also an important property controlling diffusion of solutes in soils where sorption to SOM occurs.

Acknowledgments

Specials thanks to Candida C. West (U.S. EPA, Robert S. Kerr Environmental Research Laboratories, Ada, OK) for supplying the Sleeping Bear soils and information regarding its physical/chemical properties.

Literature Cited

(1) Ball, W. P.; Roberts, P. V. *Environ. Sci. Technol.* **1991**, *25*, 1223.
(2) Ong, S. K.; Lion, L. W. *Water Res.* **1991**, *25*, 29.
(3) Piatt, J. J.; Backhus, D. A.; Capel, P. D.; Eisenreich, S. J. *Environ. Sci. Technol.* **1996**, *30*, 751−760.
(4) Chiou, C. T.; Peters, L. J.; Freed, V. H. *Science* **1979**, *206*, 831.
(5) Mingelgrin, U.; Gerstl, Z. *J. Environ. Qual.* **1983**, *12*, 1−11.
(6) Karickhoff, S. W. *J. Hydraulic Engineer.* **1984**, *110*, 707.
(7) Chiou, C. T. *Reactions and movements of organic chemicals in soils*; SSSA special publication no. 22, 1989; pp 1−29.
(8) Hassett, J. J.; Banwart, W. L. *Reactions and movements of organic chemicals in soils*, SSSA special publication no. 22, 1989; pp 31−44.
(9) Weber, W. J., Jr.; McGinley, P. M.; Katz, L. E. *Environ. Sci. Technol.* **1992**, *26*, 1955−1962.
(10) Weber, W. J., Jr.; Huang, W. *Environ. Sci. Technol.* **1996**, *30*, 881−888.
(11) Hamaker, J. W.; Goring, C. A. I.; Youngson, C. R. *Advances in chemistry series, no. 60: Organic pesticides in the environment* American Chemical Society: Washington, DC, **1966**, 23−37.
(12) Freeman, D. H.; Cheung, L. S. *Science* **1981**, *214*, 790−792.
(13) Brusseau, M. L.; Rao, P. S. C. *CRC Crit. Rev. Environ. Control* **1989**, *19*, 33−99.
(14) Pignatello, J. J. In *Reactions and Movement of Organic Chemicals in Soils*; Sawhney, B. L., Brown, K., Eds.; Soil Science Society of America: Madison, WI, 1989; pp 45−80.
(15) Brusseau, M. L.; Jessup, R. E.; Rao, P. S. C. *Environ. Sci. Technol.* **1991**, *25*, 134−142.
(16) Pignatello, J. J.; Xing, B. *Environ. Sci. Technol.* **1996**, *30*, 1−11.
(17) Jinno, K.; Kawasaki, K. *J. Chromatogr.* **1984**, *316*, 1−23.
(18) Szecsody, J. E.; Bales, R. C. *J. Contam. Hydrol.* **1989**, *4*, 181−203.
(19) Garbarini, D. R.; Lion, L. W. *Environ. Sci. Technol.* **1985**, *19*, 1122−1128.
(20) Szabo, G.; Farkas, G.; Bulman, R. A. *Chemosphere* **1992**, *24*, 403−412.
(21) Burris, D. R.; Antworth, C. P.; Stauffer, T. B.; MacIntyre. *Environ. Toxicol. Chem.* **1991**, *10*, 433.
(22) Brusseau, M. L.; Wood, A. L.; Rao, P. S. C. *Environ. Sci. Technol.* **1991**, *25*, 903−910.
(23) Brusseau, M. L.; Rao, P. S. C. *Environ. Sci. Technol.* **1991**, *25*, 1501−1506.
(24) Brusseau, M. L. *Environ. Toxicol. Chem.* **1993**, *12*, 1835−1846.
(25) Carroll, K. M.; Harkness, M. R.; Bracco, A. A.; Balcarcel, R. R. *Environ. Sci. Technol.* **1994**, *28*, 253.
(26) Holmen, B. A.; Gschwend, P. M. *Environ. Sci. Technol.* **1997**, *31*, 105−113.
(27) Xing, B.; Pignatello, J. J. *Environ. Sci. Technol.* **1997**, *31*, 792−799.
(28) Brusseau, M. L.; Rao, P. S. C. *Chemosphere* **1989**, *18*, 1691−1706.
(29) Sabljic, A. *Environ. Sci. Technol.* **1987**, *21*, 358−366.
(30) Bahnick, D. A.; Doucette, W. J. *Chemosphere* **1988**, *17*, 1703−1715.
(31) Sabljic, A.; Lara, R.; Ernst, W. *Chemosphere* **1989**, *19*, 1665−1676.
(32) Meylan, W.; Howard, P. H.; Boethling, R. S. *Environ. Sci. Technol.* **1992**, *26*, 1560−1567.
(33) Hu, Q.; Wang, X.; Brusseau, M. L. *Environ. Toxicol. Chem.* **1995**, *14*, 1133.
(34) Mackay, D.; Shiu, W. Y.; Ma, K. C. *Illustrated handbook of physical-chemical properties and environmental fate for organic chemicals*; Lewis Publishers: Chelsea, MI; Vol. 1 (1992), p 141; Vol. 2 (1992), pp 250−251; Vol. 3 (1993), pp 11−17, 622.
(35) Kier, L. B.; Hall, L. H. *Molecular connectivity in structure−activity analysis.* Research Studies Press Ltd.: Letchworth, Hertfordshire, U.K., 1986.
(36) Rao, P. S. C.; Hornsby, A. G.; Kilcrease, D. P.; Nkedi-Kizza, P. *J. Environ. Qual.* **1985**, *14*, 376−383.
(37) West, C. C.; Lyon, W. G.; Ross, D. L.; Pennington, L. K. *Environ. Geol.* **1994**, *24*, 176−187.
(38) Brusseau, M. L.; Rao, P. S. C.; Jessup, R. E.; Davidson, J. M. *J. Contam. Hydrol.* **1989**, *4*, 223.
(39) van Genuchten, M. Th. *Research Report 119*; USDA Salinity Laboratory: Riverside, CA, 1981.
(40) Piatt, J. J. Dissertation, The University of Arizona, 1997.
(41) van Genuchten, M. Th. *Memoires IAH* **1985**, *17* (1), 513−526.
(42) Park, J. K.; Bontoux, L.; Holsen, T. M.; Jenkins, D.; Selleck, R. E. *J. Am. Water Works Assoc.* **1991**, *83* (10), 71−78.
(43) Hung, G. W. C. *Microchem. J.* **1974**, *19*, 130−152.
(44) Guo, C. J.; DeKee, D.; Harrison, B. *Chem. Eng. Sci.* **1992**, *47*, 1525−1532.
(45) Ash, M.; Ash, I. *Encyclopedia of plastics, polymers, and resins;* Chemical Publishing: New York, 1982; Vol. 3, pp 138−143.
(46) Kroschwitz, J. I., Ed. In *Encyclopedia of polymer science and engineering;* Wiley & Sons: New York, 1985; Vol. 13, pp 279−284.
(47) Rutherford, D. W.; Chiou, C. T. *Environ. Sci. Technol.* **1992**, *26*, 965−970.
(48) Chiou, C. T.; Porter, P. E.; Schmedding, D. W. *Environ. Sci. Technol.* **1983**, *17*, 227.

Received for review May 27, 1997. Revised manuscript received February 13, 1998. Accepted February 19, 1998.

ES970461T